doi: 10.1038/nature06238

Radio-frequency scanning tunneling microscopy

U. Kemiktarak[1], T. Ndukum[2], K.C. Schwab[2], K.L. Ekinci[3]

[1]Department of Physics, Boston University, Boston, MA 02215 USA

[2]Department of Physics, Cornell University, Ithaca, NY 14853 USA

[3]Department of Aerospace and Mechanical Engineering, Boston University, Boston, MA 02215, USA

1-Shot Noise Thermometry and Thermal Imaging

In this section, we discuss the possibility of using the RF-STM as a local thermometer for samples that have local temperature variations on the surface. Using shot noise thermometry, one can measure the temperature of a tunnel junction very accurately in a short period of time. But there is a question that remains unanswered: What is the temperature that one would measure through shot noise thermometry, if the temperature of the STM tip is different from that of the sample? This is the situation one would encounter when imaging a sample with spatial thermal profile, such as a high density integrated circuit. Here, we provide a simple analysis towards resolving this question.

The current noise through the tip (T)-sample (S) tunnel junction is given by[1]

$$S_I(V) = \frac{2}{R}\int \left[f_T(E)\left(1 - f_S(E)\right) + f_S(E)\left(1 - f_T(E)\right)\right] dE , \qquad \text{(S1)}$$

where $f_T(E)$ and $f_S(E)$ are the Fermi-Dirac distributions for the tip and the sample. Here, temperature dependence is through the Fermi-Dirac distribution function, $f(E) = 1/\left[1 + \exp(E - \mu)/k_B T\right]$. μ is the chemical potential; in a biased tip-sample junction $\mu_S - \mu_T \approx eV_T$, where V_T is the bias voltage. Eq. (S1) can be evaluated in a

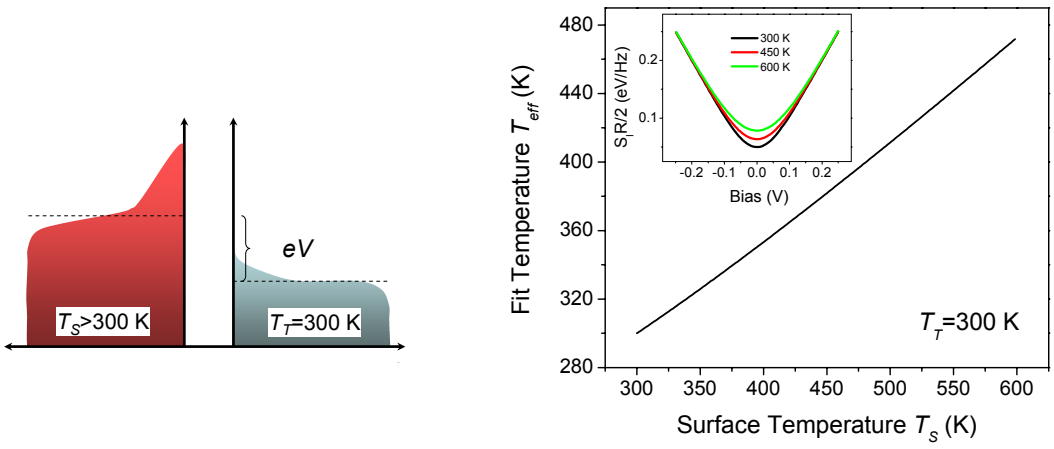

(a) **(b)**

Supplementary Figure S1. (a) Illustration of the electronic density of states for the tip and sample for the problem described in text. **(b)** Effective temperature from fits as a function of sample surface temperature when the tip is kept is at 300 K. The inset shows the change in power spectral density of current noise at several different sample temperatures with $T_T = 300$ K. Higher sample temperatures create excess noise at low bias. At high bias, all curves converge to $S_I = 2eI$ as expected. When these curves are fit to $\sim \coth(eV/2k_BT)$, as if there was no temperature difference between the tip and the sample, one gets the effective temperature T_{eff}. Note that $T_{eff} \approx (T_T + T_S)/2$.

straightforward manner to obtain $S_I(V_T) = 2eI_T \coth(eV_T/2k_BT)$ for a tunnel junction with both terminals at the same temperature.

For the case where there is a local temperature variation on the sample, we naively apply Eq. (S1) with two temperatures, i.e., $T_S = T_T(1+\theta)$ as shown in the illustration in Supplementary Fig. S1(a). Here, θ is a variable that corresponds to the fractional temperature difference. Our calculation steps can be outlined as follows: i) We first set θ $(0 \le \theta \le 1)$ with $T_T = 300$ K; ii) we calculate $S_I R_T/2$ as a function of bias

through Eq. (S1); iii) we extract the temperature from the emerging curves by fitting to $eV_T \coth(eV_T / 2k_B T_{eff})$. The extracted "effective" temperature T_{eff} is the temperature one would measure from a local hot spot on the surface. The inset of Supplementary Fig. S1(b) shows S_I as T_S is varied from 300 K to 600 K, while the tip temperature is kept constant at $T_T = 300$ K. Supplementary Figure S1(b) (main) shows the extracted fit temperature T_{eff} from this measurement. Notice that the extracted temperature from the fit is approximately the mean temperature: $T_{eff} \approx (T_T + T_S)/2$.

The averaging time for a 100×100 thermal image is obtained as follows: We take the background temperature as the sum of the ambient temperature, 300 K, and the noise temperature of our amplifier, 70 K: $T_{bg} \approx 370$ K. The measurement bandwidth is the bandwidth of the tank circuit and $B \approx 10$ MHz (half width at half maximum) as shown in Fig. 2(a). The averaging time to achieve $\Delta T \approx 1$ K temperature resolution in noise power measurement can be estimated[2] using $\Delta T / T_{bg} = 1/\sqrt{B\tau}$ as ~10 ms. In order to determine background noise and gain-bandwidth product of the system, one needs to measure the noise power as a function of bias for $eV >> 2k_B T$. Since the noise spectral density, $S_I = 2eI$, does not depend on temperature in this regime, one only needs to do this measurement once. Then measuring the noise power at a low bias value, where the temperature dependence is dominant, at every point on the surface would be enough to obtain a thermal image. Thus, an image of 100×100 points would require ~100 seconds.

2-Displacement Sensitivity and Tunneling Decay Constant:

In this section, we supply the detailed steps for obtaining an estimate for the displacement sensitivity of the RF-STM based upon the data in Fig. 3(c) and Fig. 1(b).

There are several elements in this calculation: i) the sample motion amplitude is estimated; ii) tunnel junction decay constant κ is determined; iii) the displacement sensitivity is extracted.

To estimate the displacement of the Au surface in Fig. 3(c), we first determine how much the piezoelectric actuator disk, which the Au sample is attached to, moves. Using a path-stabilized Michelson interferometer, we obtain the linear responsivity of the actuator as $\mathcal{R}=\frac{\partial z}{\partial V}\approx 0.33$ nm/V at 1 MHz. In the data presented in Fig. 3(c), the piezoelectric actuator is driven at $f_M \approx 1$ MHz at various amplitudes.

The displacement of the Au sample shaken by the piezo actuator is measured by launching a radio-frequency signal (carrier) of amplitude V_c at frequency f_{LC} towards the tank circuit, and by measuring the reflected signal amplitude V_r. Before amplification, power spectral density of the reflected signal in a single sideband is

$$\sqrt{S_{V_r}(f_{LC}\pm f_M)}\approx\frac{V_c}{2}\frac{\partial|\Gamma|}{\partial z}\bigg|_{R_T}\sqrt{S_z(f_M)}\,. \qquad \text{(S2)}$$

Here, $\sqrt{S_z(f_M)}$ represents the spectral density of displacement noise, or the available displacement sensitivity, at frequency f_M. Note that Fig. 3(c) in the main text shows the signal amplitude, $V_r(f_{LC}+f_M)$, in a 1 Hz bandwidth in the sideband divided by the carrier amplitude, $V_c(f_{LC})$. Thus, from Eq. (S2), slope of each line in Fig. 3(c) gives $\partial|\Gamma|/\partial z\big|_{R_T}$ at the particular R_T, at which the measurement is made.

R_T	$\partial\lvert\Gamma\rvert/\partial z$ (m^{-1})	$\partial\lvert\Gamma\rvert/\partial R_T$ (Ω^{-1})	κ ($Å^{-1}$)
1 MΩ	$5.76 \pm 0.89 \times 10^8$	3.9×10^{-8}	0.74 ± 0.11
2 MΩ	$3.88 \pm 0.35 \times 10^8$	1.0×10^{-8}	0.97 ± 0.088
4 MΩ	$2.29 \pm 0.25 \times 10^8$	0.26×10^{-8}	1.1 ± 0.12

Supplementary Table S1. Reflection properties and tunneling decay constants for different R_T values. $\partial\Gamma/\partial z\big|_{R_T}$ values in the first column are the slopes of the lines in Fig 3(c). In the second column, $\partial\Gamma/\partial R_T\big|_{R_T}$ values are extracted from the slope of Fig. 1(b) at the specific R_T values . κ is calculated using first two columns and the corresponding R_T values.

If an exponential tunnel junction resistance, $R_T \propto e^{2\kappa z}$, is assumed,[3] determining the decay constant, $\kappa = \frac{1}{2R_T}\frac{\partial R_T}{\partial z}$, requires the knowledge of $\partial\lvert\Gamma\rvert/\partial R_T\big|_{R_T}$ as well as $\partial\lvert\Gamma\rvert/\partial z\big|_{R_T}$. $\frac{\partial R_T}{\partial z}$ is given by $\frac{\partial R_T}{\partial z} = \frac{\partial\lvert\Gamma\rvert/\partial z\big|_{R_T}}{\partial\lvert\Gamma\rvert/\partial R_T\big|_{R_T}}$. In the experiments, $\partial\lvert\Gamma\rvert/\partial R_T\big|_{R_T}$ can be determined from the slope of the curve in Fig. 1(b) at the R_T value of interest. On the other hand, $\partial\lvert\Gamma\rvert/\partial z\big|_{R_T}$ can be determined from the slope of the lines in Fig. 3(c). The values thus obtained from the experiments are listed in Supplementary Table S1. Independent of the measurements, κ can be estimated from $\kappa = \sqrt{2m\phi}/\hbar$ where ϕ is the work function[3] if one assumes vacuum tunneling at small bias voltage. For Au, $\phi \approx 5.1$ eV and $\kappa \sim 1.16$ $Å^{-1}$, in agreement with the experiments.

Finally, we turn to the displacement sensitivity of the RF-STM. Our measurement system has a noise floor of -172.4 dBm/Hz. This is equivalent to a noise

voltage of ~5.4×10^{-10} V/$\sqrt{\text{Hz}}$ at the input of the amplifiers. The carrier power used in our measurements is -65 dBm or 130 μV. For an experimental value of $R_T \approx 1$ MΩ, we obtained $\left.\frac{\partial|\Gamma|}{\partial z}\right|_{R_T=1M\Omega} \approx 5.76 \times 10^8$ m^{-1}, from Fig. 3(c). Thus, Eq. (S2) gives minimum detectable displacement of $\sqrt{S_z} \sim 15$ fm/$\sqrt{\text{Hz}}$. If the cryogenic pre-amplifier is cooled to 4 K, the voltage noise floor goes down to ~1×10^{-10} V/$\sqrt{\text{Hz}}$, resulting in a displacement sensitivity of $\sqrt{S_z} \sim 3$ fm/$\sqrt{\text{Hz}}$. Note that the sensitivity is estimated for a small motion amplitude such that $\partial|\Gamma|/\partial z$ stays roughly constant, i.e., $z < \kappa^{-1}$.

3-Micromechancial Membrane Properties:

The silicon nitride membranes used in this study are batch fabricated using standard microlithography methods. The membrane has dimensions $w\times l\times t \approx 65$ μm × 70 μm × 40 nm (silicon nitride) and is patterned with alignment marks and coated with a 25-nm thick Au film. Scanning electron microscope (SEM) and STM images of the membrane are shown in Supplementary Fig. S2 (a) and (b).

In determining the eigenfrequencies, we assume that the membrane is perfectly flexible and very thin. We further assume that the membrane is uniformly stretched in all directions in such a way that the out-of-plane displacement of the membrane does not change its tension. In terms of the properties of the membrane, namely, its tension S, mass density ρ, thickness t, length l and width w, its resonance frequencies can be obtained as $f_{mn} = \frac{\omega_{mn}}{2\pi} = \frac{1}{2}\sqrt{\frac{S}{\rho t}\left(\frac{m^2}{w^2}+\frac{n^2}{l^2}\right)}$.

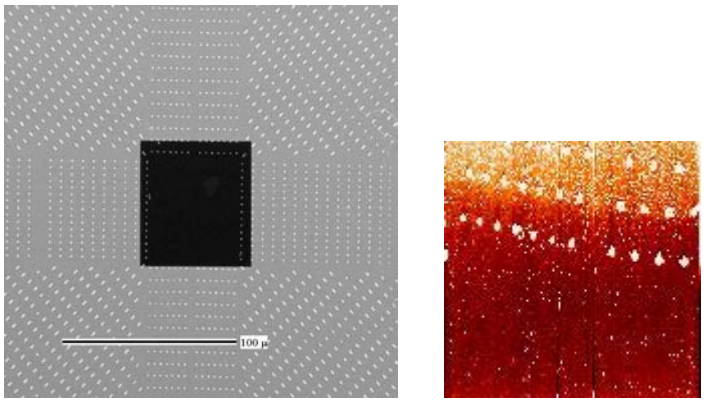

(a) **(b)**

Supplementary Figure S2. (a) Scanning electron microscope (SEM) image of the membrane used in the measurement of Fig. 3(a). We put Au markers on the chip in order to direct the STM tip towards membrane. The whole chip is covered with a 25-nm-thick Au film. **(b)** An STM image of a portion of the membrane. The markers are clearly visible. The membrane area is also recognizable as the darker region in the STM image.

1. Martin, Th., Landauer, R. Wave-packet approach to noise in multichannel mesoscopic systems. *Phys. Rev. B,* **45**, 1742 (1992).

2. Dicke, R. H. The measurement of thermal radiation at microwave frequencies. *Rev. Sci. Instrum.* **17**, 268 (1946).

3. Binnig, G., Rohrer, H., Gerber, Ch., and Weibel, E. Tunneling through a controllable vacuum gap. *Appl. Phys. Lett.* **40**, 178 (1982).